

THE GLOBULAR CLUSTER ω CENTAURI AND THE OOSTERHOFF DICHOTOMY

Christine M. Clement and Jason Rowe

Department of Astronomy, University of Toronto

Toronto, Ontario, M5S 3H8, CANADA

electronic mail: cclement@astro.utoronto.ca,rowe@astro.utoronto.ca

Received _____; accepted _____

ABSTRACT

CCD observations obtained by the OGLE team for 128 RR Lyrae variables in ω Centauri have been analysed. The period-luminosity and period-amplitude plots indicate that, in addition to fundamental (RRab) and first overtone (RRc) pulsators, the ω Centauri RR Lyrae population seems to include second overtone (RRe) and possibly third overtone pulsators. The mean period for the 59 RRab stars is 0^d.649, for the 48 RRc stars, it is 0^d.383 and for the 21 RRe stars, it is 0^d.304. The mean periods derived for the RRab and RRc stars are typical values for an Oosterhoff type II (OoII) cluster. Nevertheless, the period amplitude plot also shows that some of the RR Lyrae variables have ‘Oosterhoff type I’ (OoI) characteristics. Most of the second overtone variables exhibit non-radial pulsations similar to those recently detected in some of the RR Lyrae variables in the clusters M55 and M5, in the galactic bulge and in the LMC. Relative luminosities derived for the RRc variables from Fourier coefficients correlate with the observed apparent magnitudes. Masses for the RRc stars have been calculated from Fourier coefficients. A comparison of the derived masses for RRc stars in the four OoII clusters ω Cen, M15, M55 and M68 indicates that the masses of the RRc stars in M15 and M68 are almost $0.2M_{\odot}$ greater than those in the other two. Since M15 and M68 have a high frequency of RRd stars among their first overtone pulsators, while none have been identified in ω Cen or M55, this suggests that the double-mode pulsation phenomenon may be associated with mass. Among the RRc variables in ω Cen, the OoII variables have lower derived masses and higher luminosities than the OoI variables. An application of the period-density law to pairs of OoI and OoII RRab stars selected according to their position in the period-amplitude plot also indicates that the OoII variables in general have lower masses and higher luminosities.

These findings support the hypothesis that the RR Lyrae variables in OoII systems are evolved HB stars that spend their ZAHB phase on the blue side of the instability strip.

Subject headings: globular clusters: individual (ω Centauri) — stars: fundamental parameters — stars: horizontal-branch — stars: variables: RR Lyrae

1. INTRODUCTION

More than sixty years ago, Oosterhoff (1939) discovered that Galactic globular clusters could be classified into two groups according to the frequency distribution of the periods of their RR Lyrae variables. He suggested that the absolute median magnitude of the variables may differ from one cluster to another, but since his result was based on data for only five clusters, an extension of the investigation would be desirable. Subsequent studies by Oosterhoff (1944) and van Agt & Oosterhoff (1959) showed that the division into two groups was indeed more general.¹ At the same time, Sandage (1958) demonstrated that a difference of $\Delta M_V = 0.2$ between the RR Lyrae variables in the two groups could account for the observed difference in the periods. Meanwhile, evidence for a connection between Oosterhoff type and heavy element abundance was mounting. Arp (1955) reported that the spectra of giant stars in the OoII clusters M15 and M92 had excessively weak metal lines and Kinman (1959) reached a similar conclusion in a study of integrated spectra of globular clusters. (Kinman’s investigation was based on the spectral type obtained from a comparison of the G band with the $H\alpha$ line.) As a result of these findings, it is generally assumed that Oosterhoff type is associated with metal abundance. However, in their seminal paper on the Oosterhoff groups, van Albada and Baker (1973) pointed out that the distribution of color on the horizontal branch was a more important factor. They found that the fraction of HB stars on the blue side of the RR Lyrae gap was greater in OoII clusters. Consequently, they suggested that the RR Lyrae variables in the OoII clusters must be

¹Based on the data for 17 clusters, van Agt and Oosterhoff found that for group I (OoI) clusters, the mean period of the RRc variables $\langle P_c \rangle$ is 0^d.319, the mean period of the R Rab variables $\langle P_{ab} \rangle$ is 0^d.549, and the proportion of the variables classified as type c (n_c/N) is 0.17. The comparable figures for the OoII clusters are $\langle P_c \rangle = 0.371$, $\langle P_{ab} \rangle = 0.647$ and $n_c/N = 0.47$.

evolving from blue to red through the instability strip, while those in the OoI clusters evolve from red to blue. This difference in direction of evolution, combined with a hysteresis effect in the pulsations could account for the difference in periods and the different proportions of RRc stars between the two groups. Later, Gratton, Tornambè & Ortolani (1986) and Lee, Demarque & Zinn (1990, hereafter LDZ) pointed out that the RR Lyrae variables in the OoII clusters could be post ZAHB stars whose ZAHB phase is on the blue side of the instability strip. One would therefore expect the RR Lyrae variables in the OoII clusters to evolve redward and to have lower masses and higher luminosities than those in OoI clusters.

In Oosterhoff’s original investigations, ω Centauri was considered to belong to group II, the long period group, but when Freeman & Rodgers (1975) discovered that there was a diversity in composition among its RR Lyrae variables, some investigators recognized that it had properties of both groups. Butler, Dickens & Epps (1978) pointed out that the RR Lyrae variables with $[\text{Fe}/\text{H}]$ greater than -1 have the characteristics of type I and that the more metal poor stars exhibit type II characteristics. Taking a different approach, Caputo & Castellani (1975) demonstrated that the period-frequency plot for the low luminosity RRab stars showed OoI characteristics and suggested that ω Cen provides a link between the two Oosterhoff groups. The purpose of the present investigation is to use pulsation theory to derive relative masses for the ω Cen RR Lyrae variables to test the hypothesis that the OoII variables have lower masses and higher luminosities than the OoI variables. Our study is based on the observations made by the OGLE team.

2. THE OGLE DATA FOR RR LYRAE VARIABLES IN ω CENTAURI

2.1. Light curves, period-luminosity and period-amplitude relations

In 1993, 1994 and 1995, CCD observations of ω Centauri were made as a side-project of the OGLE (Optical Gravitational Lensing Experiment) team. As a result, three papers on variable stars have been published by Kaluzny and his collaborators (Kaluzny *et al.* 1996, 1997a, 1997b). The first two papers deal with eclipsing binaries, SX PHe stars and spotted variables, and the third, hereafter referred to as K97b, presents periods and light curves for 140 RR Lyrae and population II Cepheid variables.

The present investigation is based on the V magnitudes for 128 of the stars studied by K97b. Our sample consists of all of the stars with mean V magnitude between 14.0 and 15.2 and periods less than 0^d.9, with the exception of OGLE# 95, 96, 171 and 208 for which K97b published periods close to one half day and amplitudes less than 0.2 mag. The OGLE observations included seven different fields: 5139A, B, C, BC, D, E and F. Field 5139B, which covered the most central part of the cluster, contained more RR Lyrae variables than any of the other fields, but many of these stars were included in other fields as well. Since there are zero point shifts as large as 0.05 mag from one field to another, it was desirable to consider as many stars as possible in one field only. Consequently, if a star was observed in field B, our analysis is based only on the observations in field B. Some stars were observed only in fields E and F, and in these cases, we used the data from field E. In general, we included only magnitudes for which the listed error was less than 0.02 mag for our analysis. However, for OGLE #194, we included all magnitudes with errors less than 0.03 in order to obtain sufficient phase coverage..

To begin our analysis, we plotted a light curve for each star using the period listed in Table 1 of K97b. For some stars, we found small phase shifts in the curves, and in these cases, we revised the periods. Our adopted periods are listed in Table 1 and light curves, arranged in order of increasing period, are shown in Figure 1. All but one of the periods

agree to within 0^d0001 of those published by K97b. For star OGLE #149, we found a much shorter period, 0^d378 compared with the K97b value 0^d609 . An examination of Fig. 1 shows how the general characteristics of the light curves change with period. It was in a study of the RR Lyrae variables in ω Cen that Bailey (1902) set up his three subclasses *a*, *b* and *c*. He considered V8 (OGLE # 199, $P=0^d5213$) to be a typical star for subclass *a*, V3 (OGLE #184, $P=0^d84126$) for subclass *b* and V35 (OGLE #78, $P=0^d3868$) for subclass *c*. The stars of subclass *c* have the shortest periods and type *b* have the longest periods. In addition, the light curves for the three subclasses differ in amplitude and in shape. It was subsequently demonstrated by Schwarzschild (1940), in a test of the period-density relation for RR Lyrae variables in M3, that the *c*-type variables were most likely pulsating in the first overtone, while the *a*- and *b*- types were pulsating in the fundamental mode. Since this mode difference was recognized, the distinction between *a* and *b* has usually been disregarded and both groups have been referred to as RRab types. However, because of the high quality of the light curves of Fig. 1, the difference between types *a* and *b* is very clear. There is a sudden change in slope about halfway up the rising branch of the *b* type light curves. Other stars classified as *b* by Bailey and subsequently by Martin (1938) in his major study of ω Cen are variables 15, 26, 34, 38, 54 and 85 (OGLE # 124, 120, 90, 170, 74 and 176 respectively) and the light curves for all of these stars show that same characteristic.

In Table 1, we list for each star the OGLE ID#, the variable number from Sawyer Hogg’s (1973) catalogue,² the field, our adopted period, the *V* amplitude, the mean *V* magnitude and the mode of pulsation according to the location of the star in the period-amplitude diagram. The period-luminosity (P-L) and period-amplitude (P-A) relations are plotted in Fig. 2. The points in the P-A diagram seem to fall into different regimes which we interpret to be due to different modes of pulsation and have therefore

² OGLE # 191 and #71 (V184 and V185) were discovered by Butler *et al.* (1978).

plotted a different symbol for each mode. Also, among the fundamental mode and second overtone pulsators, there are two sequences in the P-A plot. A mean magnitude of 14.65 roughly divides the stars into these two sequences. We assume these occur because stars of both Oosterhoff classes are present in ω Cen. This will be discussed further in section 3. In Table 1, the fundamental mode pulsators are denoted as F and the overtone pulsators as 1st, 2nd or 3rd, depending on the mode of pulsation. The amplitudes and mean magnitudes listed in Table 1 were obtained from fits of the V magnitudes to a Fourier series of the form:

$$mag = A_0 + \sum_{j=1,n} A_j \cos(j\omega t + \phi_j) \quad (1)$$

where ω is $(2\pi/\text{period})$. For each star, the epoch was taken as HJD 2449000.000 so that t in the equation refers to $(\text{HJD}-2449000.000)$ and HJD represents the heliocentric Julian date of the observation.³ For the fundamental mode pulsators, the order of the fit n was 8 and for the overtone pulsators, it was 6. The adopted mean V magnitude is A_0 from the fit of equation 1. In order to classify the light curves of the fundamental mode pulsators as normal (n) or peculiar (p), we used equations derived by Kovács & Kanbur (1998) for testing the compatibility condition of Jurcsik & Kovács (1996, hereafter JK).

The mean periods for the stars in our sample are as follows: 0^d.649 for the 59 fundamental mode, 0^d.383 for the 48 first overtone and 0^d.304 for the 21 second and third overtone pulsators. The mean periods for the fundamental and first overtone are very close to those derived by van Aagt and Oosterhoff (1959) for the Oosterhoff type II clusters. Thus, even though ω Cen seems to contain RR Lyrae variables of both Oosterhoff groups, most belong to group II.

³OGLE #71 and #119 have periods very close to 0^d.33 and as a result, the phase coverage was not complete. However, for both of these stars, the maximum and minimum on the light curve were well defined and so we estimated the amplitude from these.

2.2. Evidence for Second Overtone Pulsation

Although we have classified many of the RR Lyrae stars as second overtone pulsators (RRe stars), the possibility of the existence of RRe stars has been the subject of some debate in the literature. A few years ago, Stellingwerf, Gautschy & Dickens (1987) calculated a model for a second-overtone pulsator with an amplitude similar to first overtone pulsators. They predicted that the light variation of an RRe star should have a sharper peak at maximum light. However, they noted that they could not exclude the possibility that RRe stars may have lower amplitudes and sinusoidal light variations. The RRe candidates that we have identified in ω Cen have sinusoidal light variations and low amplitudes compared to the fundamental mode and first overtone pulsators. This is illustrated in Figure 3 where we show the light curves for the three stars that Bailey considered the prototypes for his subclasses *a*, *b* and *c* along with the curve for OGLE #191 (V184), one of the stars we have classified as RRe. There is a distinct progression in amplitude and degree of symmetry from subclass *a* through *c* and #191 forms a natural extension to the sequence.

Studies of P-A relations have led many other investigators to recognize plausible RRe candidates. Evidence for an RRe star in the field (V2109 Cygni) has been presented by Kiss *et al.* (1999). Credible RRe candidates have also been identified in the globular clusters M68 (van Albada & Baker 1973), NGC 4833 (Demers & Wehlau 1977), IC 4499 (Clement, Dickens & Bingham 1979, Walker & Nemec 1996), M3 (Kaluzny *et al.* 1998, hereafter K98) and M5 (Kaluzny *et al.* 2000, hereafter K2000). In addition, recent studies of M2 (Lee & Carney 1999a) and NGC 5466 (Corwin, Carney & Nifong 1999) indicate that there may be second overtone pulsators in these clusters as well. However, Kovács (1998a) compared the RRe candidates in M68 and IC 4499 with the other RRc stars and concluded that their relative magnitudes and colors were incompatible with the assumption that they were RRe stars. Furthermore, the models of Bono *et al.* (1997, hereafter referred to as B97)

predict that a plot of amplitude versus period (or temperature) for first overtone pulsators shows a characteristic ‘bell’ shape with amplitudes decreasing at shorter periods and higher temperatures. One would therefore expect the first overtone variables with the shortest periods to have the lowest amplitudes. This is exactly what Clement & Shelton (1999a) found in a recent study of the globular cluster M9; the P-A plot for the overtone pulsators had the classic ‘bell’ shape. Thus, it is possible that some of the short-period, low-amplitude variables in ω Cen are pulsating in the first overtone mode. Nevertheless, we believe that the shifts in the period-luminosity plot for the stars in the different period-amplitude regimes of Fig. 2 indicate the existence of more than two pulsation modes. Among the stars plotted in the upper panel of Fig. 2 with $\langle V \rangle$ between 14.5 and 14.65, the RRe candidates (solid triangles) have $\log P$ in the range -0.55 to -0.45 while the other RRc stars (open circles) have longer periods ($\log P$ between -0.45 and -0.35). The luminosities of both groups are comparable. RRe stars are expected to have shorter periods and lower amplitudes so we might assume that the stars with shorter periods are RRe stars. On the other hand, if they are all RRc stars, the stars with shorter periods must have higher temperatures and/or higher masses. This is required by the period-density relation (see equation (7)). If the temperatures are the same, the stars with shorter periods must have higher masses. However, when we consider the amplitudes, it turns out that the short period stars can not have higher masses. B97 made a number of plots to illustrate the dependence of amplitude for first overtone pulsators on temperature, mass and luminosity. Their diagrams demonstrate that, at constant temperature and luminosity, stars with lower amplitudes have lower not higher masses. This implies that if the solid triangles represent first overtone pulsators, they must have higher temperatures than the others. In fact, they must be hotter by $\Delta \log T_e \sim 0.029$ (almost 500K). Another puzzling feature to note in the period-amplitude plot of Fig. 2 is the general tendency for amplitude to decrease with increasing period for the solid triangles brighter than $\langle V \rangle = 14.65$. This is not the

characteristic ‘bell’ shape predicted by B97 for period amplitude plots of first overtone variables. We therefore conclude that these stars are probably not first overtone pulsators; rather they are pulsating in the second overtone mode. There may even be third overtone pulsators among the RR Lyrae population in ω Cen!

Most of the second and third overtone pulsators listed in Table 1 have no Sawyer Hogg numbers. This is because their amplitudes are generally lower than those of the RRc stars and as a result, they were not identified in the earlier photographic studies of ω Cen by Bailey (1902) and Martin (1938). It is also possible that the four stars that we excluded from our investigation, OGLE #95, 96, 171 and 208 are second overtone pulsators.

An independent argument for the existence of RRe stars has been proposed by the MACHO consortium. In a study of RR Lyrae variables in the LMC, Alcock *et al.* (1996) showed that the period frequency distribution had three peaks, at periods of 0^d.58, 0^d.34, and 0^d.28 respectively. They interpreted this to mean there were three pulsation modes. In Fig. 4, we plot a period-frequency distribution for the OGLE sample of ω Cen RR Lyrae variables. It also has three peaks, but the periods associated with the peaks are longer than those in the LMC. They occur at periods of 0^d.63, 0^d.40 and 0^d.32. We assume that the periods for the peaks differ because most of the RR Lyrae variables in ω Cen have OoII characteristics, while the LMC has mainly an OoI population. An examination of Figure 2 shows that, although there are some RRc stars with periods of approximately 0^d.32 ($\log P = -0.49$), the peak would not occur if there were no RRe stars. We therefore concur with Alcock *et al.* that the reason for the extra peak at short periods in the period-frequency distribution of both systems is the presence of RRe stars. There is another important difference between the period-frequency distributions of ω Cen and the LMC – the size of the peaks. For ω Cen, they are all at approximately the same height, but for the LMC, the height of the peak increases with period, thus implying there are more

RRab stars than RRc stars and more RRc stars than RRe stars. It is well known that OoI systems have more RRab stars than RRc stars and van Albada and Baker (1973) attributed this to different predominant directions of evolution through the instability strip for the two groups, accompanied by a hysteresis effect in the pulsation. This could account for the fact that the LMC has significantly fewer RRe stars than RRc stars. However, it may also be a detection problem because the RRe stars have lower amplitudes.

2.3. Evidence for Non-Radial Pulsations

With accurate CCD photometry, it is possible to identify low level changes in the amplitudes of RR Lyrae variables and a number of such changes have been noted. Walker (1994) found short term variations in the light curve of the short period RRc (RRe candidate) star V5 in M68. More recently, Olech and his collaborators found changes on time scales of a few days in the light curves of three RRc stars in M55 (Olech *et al.* 1999a) and one in M5 (Olech *et al.* 1999b). They also found that these stars all had multiple periods. For example, in their analysis of V104 in M5, they identified two clear peaks in the periodogram at periods of 0^d.332 and 0^d.311 and they attributed these to the presence of non-radial oscillations, similar to those observed in many δ Scuti stars. Theoretical calculations made by Van Hoolst *et al.* (1998) have demonstrated that non-radial modes can be excited in RR Lyrae variables as well. Non-radial oscillations have also been detected in some RR Lyrae stars in the Galactic Bulge by Moskalik (2000) and in the LMC by Kovács *et al.* (2000).

The OGLE dataset for ω Cen includes a number of RR Lyrae stars that change on a time scale of days. In particular, K97b commented on the instability of the light curve of #162, but an examination of the light curves of Fig. 1 indicates that there are others as well. In Fig. 5, we show a light curve for #186, based on 10 consecutive nights in 1995.

The observations for each night are plotted with a different symbol and it is very clear that there are changes on the scale of a few days. In Fig. 6, we present Θ -transforms for #186; the real data are plotted in the upper panel and the prewhitened data in the lower panel. The diagram indicates that there are two well defined periods, just as Olech *et al.* found for the stars that they studied. Thus we conclude that #186 is an RRe star that exhibits non-radial pulsations.

2.4. Physical Properties derived from Fourier parameters

2.4.1. RRc stars

In the last few years, two methods have been devised for deriving luminosities of RR Lyrae variables from Fourier parameters. Since there is a range of more than 0.5 in the apparent V magnitude among the RR Lyrae variables in ω Cen, it provides a good sample for testing these methods.

In an investigation of hydrodynamic pulsation models for RRc stars, Simon & Clement (1993a,b) analysed the light curves and derived the following relationships:

$$\log L/L_{\odot} = 1.04 \log P - 0.058\phi_{31} + 2.41 \quad (2)$$

$$\log M/M_{\odot} = 0.52 \log P - 0.11\phi_{31} + 0.39 \quad (3)$$

where L/L_{\odot} is the luminosity in terms of the Sun's luminosity, M/M_{\odot} is the mass in solar units, P is the pulsation period in days, ϕ_{31} is the Fourier phase difference ($\phi_3 - 3\phi_1$) computed from the fit of equation (1) to the points. (The standard deviations of the fits for $\log L/L_{\odot}$ and $\log M/M_{\odot}$ to equations (2) and (3) were $\sigma = 0.025$ and 0.03 respectively.) Thus the analysis indicated that ϕ_{31} depends essentially on mass and luminosity and that it is insensitive to metallicity. This means that equations (2) and (3) can be applied to stars

with different metal abundance. Once the mass and luminosity have been evaluated, the effective temperature can also be calculated from the period-density relation which can be expressed in the following form:

$$\log T_e = 3.265 - 0.3026 \log P - 0.1777 \log M/M_\odot + 0.2402 \log L/L_\odot \quad (4)$$

Kovács and his collaborators took a different approach. They derived empirical formulae for calculating M_V by studying systems in which there are large numbers of RR Lyrae variables, e. g. the Sculptor dwarf galaxy. For the RRC stars, Kovács (1998b) derived the following formula for calculating the absolute magnitude:

$$M_V = 1.261 - 0.961P - 0.044\phi_{21} - 4.447A_4 \quad (5)$$

where P is the period, ϕ_{21} is the phase difference ($\phi_2 - 2\phi_1$) based on a sine series fit, A_4 is the fourth order amplitude and the standard deviation of the fit was 0.042. The zero point was based on the Baade-Wesselink luminosity scale of Clementini *et al.* (1995). It should be noted that the luminosity scale for RR Lyrae variables is still the subject of some controversy, but even if there is an error in the zero point for equation (5), the relative ranking of the magnitudes will not be affected.

In Table 2, we list the Fourier phase differences ϕ_{21} , ϕ_{31} , (along with their errors) and the amplitude A_4 for all of the overtone pulsators derived from equation (1). Also included are M_V , $\log L/L_\odot$ and M/M_\odot calculated from equations (2), (3) and (5) and $[\text{Fe}/\text{H}]_{hk}$ values recently determined by Rey *et al.* (2000, hereafter R2000) from *Caby* photometry. The stars are arranged in order of increasing period. The asterisks beside some of the star numbers refer to the Oosterhoff type and will be discussed further in section 3.1. In our calculations of M_V , $\log L/L_\odot$ and M/M_\odot , we included only the stars for which the error in the phase difference is less than 0.2. For most of the short-period stars, the errors are large, particularly those for ϕ_{31} . This is because of their low amplitudes and sinusoidal light

curves. Kovács’ Fourier fit was based on a sine series, but the parameters that we list in Table 2 are based on a cosine series. Therefore, to put our values for the phase differences on the same system as his, we subtracted 1.57 from ϕ_{21} before we computed M_V . In Fig. 7, we plot the computed $\log L$ and M_V against the mean V magnitude. The first overtone pulsators are plotted as solid circles and the second overtone pulsators as open triangles. The crosses represent stars not considered to be cluster members. The open circles enclosed in boxes denote four anomalous variables #132, #169 (V123), #185 (V47) and #73 (V68) which all have unusually high values of ϕ_{21} according to Table 2. We have classified them as RRc stars even though they all have periods greater than 0^d.44. The envelope lines in the upper panel are separated by $\Delta V = 0.12$, the uncertainty in the calibration of equation (2) and most of the solid circles lie either on these lines or between them. It appears that equation (2) is effective for predicting the relative luminosities of the RRc stars. The envelope lines in the lower panel are separated by 0.085, the uncertainty in Kovács’ (1998b) calibration and here the fit is not quite so good. For the faintest first overtone pulsators, the predicted magnitudes are too bright. On the other hand, equation (5) predicts fainter values of M_V for the second overtone pulsators due to their shorter periods and lower A_4 . No values of $\log L$ were computed for second overtone pulsators because the errors in their ϕ_{31} values were all greater than our threshold 0.2 because of their low amplitudes.

In Fig. 8, we show the relationship between $\log L$ and M_V calculated from the Fourier parameters. They correlate well and this leads us to conclude that the two outliers plotted as crosses in Fig. 7 at $M_V \sim 0.8$ (#97 and #192) are not cluster members. They just happen to be in the field of view. Another star that is probably not a member is #181 which, with $\langle V \rangle = 15.181$, is off the scale of Fig. 7. However, it is plotted in Fig. 8 and lies between the envelope lines. The outlier at $M_V = 0.477, \log L = 1.77$ in Fig. 8 is star #185 (P=0^d.485), one of the anomalous stars with large ϕ_{21} . The light curve for this star has an inflection on the rising branch that is different from most of the other RRc stars. The

light curve for #169 is similar, but it is not plotted in Fig. 8 because its ϕ_{31} error is greater than 0.2. If it were, the point would also lie to the right of the envelope lines.

2.4.2. *RRab stars*

An empirical formula for relating the absolute magnitude to period and Fourier coefficients for RRab stars was derived by Kovács & Jurcsik (1996):

$$M_V = 1.221 - 1.396P - 0.477A_1 + 0.103\phi_{31} \quad (6)$$

In Table 3, we list the Fourier amplitude A_1 , phase difference ϕ_{31} , M_V calculated from equation (6) for the RRab variables with ‘normal’ light curves and the $[\text{Fe}/\text{H}]_{hk}$ values recently determined by R2000. The stars are listed in order of increasing period. The Fourier coefficients in equation (6) are based on a sine series. Therefore, to put our coefficients from Table 3 on the appropriate system, we added 3.14 to ϕ_{31} before calculating M_V . In Fig. 9, we plot M_V against $\langle V \rangle$ and the two quantities correlate reasonably well. However, the fit for the ω Cen RRab stars is not as good as the fits for NGC 6171 and M3 based on the observations of Clement & Shelton (1997) and Kaluzny *et al* (1998). The envelope lines have a slope of unity and their separation $\Delta V = 0.1$ represents the uncertainty in the values of M_V derived from equation (6). Most of the points fall between the two lines, but #174 (V84) with $\langle V \rangle = 14.291$ is displaced by more than 0.3 mag. Bailey did not determine a period for this star, but in Fig. 1, it is clear that its light curve has the classic ‘b’ characteristics in spite of its relatively short period (0^d5799). In their paper on the chemical inhomogeneity of ω Centauri, Freeman & Rodgers (1975) found that the strength of the Ca II K-line for this star was greater than that of any of the other 27 RR Lyrae variables in their sample. We therefore conclude that #174 (V84) is a foreground star that belongs to a different population.

3. THE OOSTERHOFF DICHOTOMY IN ω CENTAURI

3.1. The Period-Amplitude Relation

In a study of the period-amplitude relation of RRab stars in the OoI globular clusters M107, M4, M5, M3, and the OoII clusters M9, M68 and M92, Clement & Shelton (1999b) found that the period-amplitude relation for RRab stars appears to be a function of Oosterhoff type. They therefore concluded that evolutionary effects were more important than metal abundance for determining where a star lies in the period-amplitude plane provided the star had a ‘normal’ light curve. In Fig. 10, we plot A_V versus $\log P$ for the ω Cen fundamental mode pulsators with ‘normal’ light curves and for first overtone stars with errors less than 0.2 in ϕ_{31} . Only stars that are considered to be members of the ω Cen population according to the discussion in sections 2.4.1 and 2.4.2 are included in the plot. Stars with $\langle V \rangle \leq 14.65$ are plotted as solid triangles or solid circles and the fainter stars are plotted as open triangles or open circles. The straight line between $\log P = -0.24$ and -0.05 is a least squares fit to the RRab stars with $\langle V \rangle \leq 14.65$ and its location in the P-A plane is close to the line that Clement & Shelton (1999b) derived for OoII RRab stars. Most of the (solid) points lie very close to this line; their mean deviation $\langle \Delta \log P \rangle$ is 0.014. Their mean period is $0^{\text{d}}673$, a value appropriate for an OoII classification. Jurcsik (1998a) has previously pointed out that the bulk of the RRab stars in ω Cen comprise a very homogeneous group and one can see this in Fig. 10. The straight line between $\log P = -0.32$ and -0.14 is the OoI P-A relation that Clement & Shelton (1999b) derived from the M3 data of K98. Several of the fainter RRab stars (the open circles and the open triangles) lie close to this OoI relation. The mean period for the fainter stars is $0^{\text{d}}542$, a typical OoI value. Thus the P-A relation for the RRab seems to be effective for distinguishing between Oosterhoff types. The fainter RRab stars are more metal rich on the average; their mean $[\text{Fe}/\text{H}]$ is -1.53 compared with -1.74 for the stars with $\langle V \rangle \leq 14.65$.

However, there is not a strong correlation between $\langle V \rangle$ and $[\text{Fe}/\text{H}]$. This point has already been made by R2000 and by Demarque *et al.* (2000) who note that the luminosity also depends on evolutionary status or HB morphology.

The other lines in Fig. 10 represent least squares fits to the P-A relations for the RRc stars in M3 (OoI) and M68 (OoII) based on the data of K98 and Walker (1994). In this case, the distinction between OoI and II is not so marked for stars brighter or fainter than 14.65. It seems that, for the RRc stars, the $\langle V \rangle = 14.65$ cutoff distinguishing between OoI and OoII types is too faint. Therefore, in our discussion of RRc stars in the next section, we decide Oosterhoff type according to position in the P-A diagram. RRc stars with periods less than $0^{\text{d}}35$ lie closer to the M3 line and so we consider them to be OoI variables. Stars with periods in the range $0^{\text{d}}35$ to $0^{\text{d}}43$ are considered to be OoII variables. The OoI stars are indicated by single asterisks and the OoII stars by double asterisks in Table 2.

A curious feature of Fig. 10 is the existence of first overtone pulsators with periods in the range of $0^{\text{d}}44$ to $0^{\text{d}}54$. M68 does not have any overtone pulsators with such long periods, even among the double-mode pulsators whose first overtone periods range from $0^{\text{d}}39$ to $0^{\text{d}}41$. These long period stars in ω Cen are brighter than the others and as we noted in section 2.4, they have unusually large values for ϕ_{21} . The stars with the inflection on the rising branch of the light curves (#169 and #185) are among them. The recent study of M5 by K2000 shows that M5-V76 has similar properties.

3.2. The Masses and Luminosities of the RRc stars

In section 2.4.1, we showed that equation (2), which was derived from hydrodynamic pulsation models by Simon & Clement (1993a), successfully ranks the relative luminosities

of the ω Cen RRc stars. K2000 reached the same conclusion in their recent study of M5. We now use the masses computed from equation (3), which was also derived from the models, to compare the masses and luminosities of RRc stars in clusters belonging to both Oosterhoff groups. Our results are summarized in Table 4 where we compare the data for ω Cen with six other well studied globular clusters, three from each Oosterhoff group. These are M107 (Clement & Shelton 1997), M5 (K2000), M3 (K98), M55 (Olech *et al.* 1999a), M68 (Walker 1994) and M15 (Clement & Shelton 1996, based on the data of Silbermann & Smith 1995). For each cluster, we list $[\text{Fe}/\text{H}]$, the number of stars analysed, their mean period, mean mass, mean luminosity and mean temperature. For these last three quantities, we also include the standard error of the mean. Most of the $[\text{Fe}/\text{H}]$ values are taken from the compilation of Zinn (1985), but for ω Cen, they are means of the $[\text{Fe}/\text{H}]_{hk}$ values derived for the individual stars by R2000. The ω Cen variables are segregated according to Oosterhoff type. The four bright stars with periods greater than $0^{\text{d}}44$ are not included. Their derived masses are uncertain because they are well below the range of the models which were computed for masses ranging from 0.55 to $0.85M_{\odot}$. The clusters are arranged in order of increasing $\log L/L_{\odot}$ which is, in general, the order of decreasing metal abundance and decreasing temperature. The mean period increases through the sequence until M68 and M15, the two OoII clusters that have the highest frequency of double-mode RR Lyrae variables (RRd stars).⁴ In these two clusters, the overtone pulsators with periods longer than $0^{\text{d}}39$ are RRd stars and as a result, the mean periods for their RRc stars are shorter than those for M55. The masses calculated from equation (3) are low compared with those derived from evolutionary models (Dorman 1992) and other investigations of pulsation. However, the relative ranking is in agreement with masses derived from the analysis of

⁴Recent CCD observations of the RRd stars in M68 and M15 have been published by Walker (1994) and Purdue *et al.* (1995) respectively.

RRd stars. Studies of pulsation models by Kovács *et al.* (1992), Cox (1995) and Bono *et al.* (1996) all indicate that the RRd variables in the OoII clusters M15 and M68 are more massive than those in the OoI clusters M3 and IC 4499. Most of their models indicate that the difference between the two is approximately $0.1M_{\odot}$. Three of these clusters are included in Table 4 which indicates that the RRc stars in M15 and M68 are $0.13M_{\odot}$ more massive than the ones in M3. Another point to note about M68 and M15 is that the masses derived for their RRc stars from ϕ_{31} are considerably higher than those for ω Cen and M55. If this is correct, then the data of Table 4 suggest that the double-mode phenomenon may occur only in higher mass stars. Recent studies of M55 and ω Cen have not revealed any RRd stars. Furthermore, Nemec, Nemec & Norris (1986) analysed Martin’s (1938) published observations of the ω Cen RR Lyrae variables and found no RRd stars. Freyhammer, Andersen & Petersen (1998, 2000) have detected multi-mode pulsation in a few variables in ω Cen, but they are SX Phe, not RR Lyrae variables.

Another feature of the sequence of masses listed in Table 4 is the discontinuity at the interface between the two Oosterhoff groups. Although there is an increase of mass with luminosity among the clusters in each group, there is a sudden drop in mass at the transition. The OoII RRc stars in ω Cen and M55 have lower masses and higher luminosities than the OoI RRc stars in ω Cen and M3. This is exactly what is predicted by LDZ. The OoII RR Lyrae variables are evolved stars from the blue horizontal branch so that when they cross the instability strip, they have lower masses and higher luminosities than the OoI variables.

3.3. The Masses of the RRab stars

We now use the period-density relation to compare the masses of the RRab stars of the two Oosterhoff groups in ω Cen. The period-density relation can be expressed as a

relationship among pulsation period, luminosity, mass and surface effective temperature. From models based on OPAL opacities, Cox (1995) derived a relation for fundamental mode RR Lyrae pulsators with composition comparable to the ω Cen variables ($Z=0.0003$):

$$\log P = 11.519 + 0.829 \log L/L_{\odot} - 0.647 \log M/M_{\odot} - 3.479 \log T_e \quad (7)$$

Our procedure is to select pairs of stars for which the amplitude is the same (within 0.02 mag), one from each Oosterhoff group according to the P-A diagram of Fig. 10, and then use the period-density relation to calculate the difference in mass. From equation (7), we derive:

$$0.647 \Delta \log M/M_{\odot} = -0.332 \Delta m_{bol} - \Delta \log P - 3.479 \Delta \log T_e \quad (8)$$

where m_{bol} refers to the apparent bolometric magnitude. We limit our selections to pairs of stars in the same field so that the luminosity difference obtained from the observations is reliable. Otherwise the shifts in zero point between the different fields would introduce large uncertainties into the results.

In order to apply equation (8), we need to know the temperature differences, but the temperatures of the stars are not known. Our approach therefore is to evaluate $\Delta \log M/M_{\odot}$ for three different assumed values of $\Delta \log T_e$, selected in the following manner. We choose our first value $\Delta \log T_e = 0.000$ because B97 showed that the correlation between amplitude and effective temperature of fundamental mode pulsators does not have a strong dependence on mass or luminosity. Their study was based on nonlinear pulsation models with helium content $Y = 0.24$. On this basis, one would expect a one-to-one correspondence between amplitude and temperature. Our second value for $\Delta \log T_e$ is -0.004 . We choose this value because Sandage (1993) presented evidence that OoII RRab stars are cooler than those of OoI. For RRab stars at the blue fundamental edge of the instability strip, he derived the relationship: $\Delta \log T_e = 0.012 \Delta [Fe/H]$. Among the star pairs we have selected, the

OoII RRab stars are more metal poor by an average amount -0.34 . Therefore, based on Sandage’s relationship, we derive a mean $\Delta \log T_e = -0.004$. We choose our third value -0.005 because our analysis of the RRC stars in ω Cen also indicates that the OoII RR Lyrae variables are cooler. According to the data of Table 4, the mean temperature of the OoII RRC stars in ω Cen is lower by $\Delta \log T_e = 0.005$ than that of the OoI stars. For equation (8), we also need to know the bolometric corrections (BC) in order to compute m_{bol} . Jurcsik (1998b) derived equations for relating BC to $[\text{Fe}/\text{H}]$ and temperature and from her equations, we derive the following relationship:

$$\Delta BC = 1.56115 \Delta \log T_e + 0.0445 \Delta [\text{Fe}/\text{H}]. \quad (9)$$

We use equation (9) to calculate ΔBC for each assumed value of $\Delta \log T_e$.

Our selected pairs of stars (seven in all) are listed in Table 5. Also listed are the observed differences $\Delta \log P$, ΔV , ΔA_V and $\Delta [\text{Fe}/\text{H}]$ and the $\Delta \log M$ values calculated from equation (8) according to the different assumptions for $\Delta \log T_e$. On the last line, the mean value for each quantity is listed. For each assumed temperature difference, the mean mass of the OoII stars is lower than the mean for the OoI stars, just as we found for the RRC stars. This is further support for the LDZ hypothesis. If the LDZ hypothesis is correct, one would also expect to find that the periods of OoII RR Lyrae stars increase. This is exactly what has been found in a recent study of the period changes of RRab stars in ω Cen by Jurcsik (2000) and Jurcsik *et al.* (2000).

Although our analysis of the RRab star pairs indicates that, in general masses are lower and luminosities are higher for the OoII stars, there are individual cases that are exceptions. For example, the OoII star #147 has a higher mass than the OoI star #154 for all of our assumed values of $\Delta \log T_e$. This is because #147 is so much brighter than #154 that its mass must also be larger to account for its observed period. Another anomalous star is #113. For six of the seven pairs listed in Table 5, the OoII star is brighter, but

the OoI star #113 is brighter than its OoII counterpart. In fact, it is brighter than any of the other stars that lie near our adopted OoI P-A relation. An examination of Fig. 1 shows that its light curve does not have the characteristic bump and dip preceding the rise to maximum light. Theoretical light curves published by B97 illustrate that, at constant mass and temperature, models with higher luminosity have a less pronounced bump. This is exactly what we observe in the light curve of #113. It may have a mass and temperature similar to the other OoI stars, but it is more luminous. With high quality light curves based on CCD observations, it is becoming possible to distinguish between different models.

4. The Origin of the Dichotomy

Our analysis of the RR Lyrae stars in ω Cen has confirmed that the cluster contains variables with the properties of both Oosterhoff groups. We have also presented evidence to illustrate that both the RRc and RRab OoII variables belong to a more evolved population than the OoI variables. On the average, the OoII variables are less massive, more luminous stars that have spent their ZAHB phase on the blue side of the instability strip. The same conclusion can be reached from a comparison of the first overtone pulsators in the OoI cluster M3 and the OoII cluster M55. One explanation for this advanced evolutionary state is that their ZAHB masses are low because of a high mass-loss rate at the tip of the red giant branch. Alternatively, it could be that the masses of their main sequence progenitors are lower and consequently, the OoII variables are older. This is the conclusion that Lee & Carney (1999b) reached in their investigation of M2 and M3, two clusters that have similar metallicities, but different Oosterhoff types. By comparing the difference in color between the base of the giant branch and the main sequence turnoff, they estimated that the OoII cluster M2 is about 2 Gyr older than the OoI cluster M3. It is possible that the Oosterhoff dichotomy in ω Cen is also due to an age difference. Recent studies of ω Cen by Hilker &

Richtler (1999) and Hughes & Wallerstein (2000) present evidence for a range in age of at least 3 Gyr. Both groups performed Strömgren photometry (Hilker & Richtler observed red giants and Hughes & Wallerstein observed stars near the main sequence turnoff) and both found that the more metal rich stars are at least 3 Gyr younger. The data listed in Tables 4 and 5 of the present paper indicate that the OoI RR Lyrae variables in ω Cen are more metal rich than the OoII variables. Thus if the age-metallicity correlation can be extended to HB stars, a difference in age may be the cause of the Oosterhoff dichotomy in ω Cen. An examination of Dorman’s (1992) oxygen-enhanced models for HB stars with $[\text{Fe}/\text{H}]=-1.48$ and -1.66 (metallicities comparable to those observed in the ω Cen RR Lyraes) shows that at $\log T_e = 3.86$ (a temperature appropriate for the instability strip), there are models with $[\text{Fe}/\text{H}] = -1.66$ and $\log L = 1.74$ that are less massive than models with $[\text{Fe}/\text{H}]=-1.48$. However, the mass difference between the two is less than $0.01M_\odot$. The mass differences listed in Tables 4 and 5 are greater. Clearly, there is still more work to be done before we can fully understand the evolution of RR Lyrae variables and the Oosterhoff dichotomy.

We would like to thank Giuseppe Bono, Bruce Carney, Marcio Catelan, Johanna Jurcsik, Andy Layden, Geza Kovács, Joergen Petersen, Robert Rood, Horace Smith and Allen Sweigert for discussing this work during the course of the investigation. Support for this work from the Natural Sciences and Engineering Research Council of Canada is gratefully acknowledged.

REFERENCES

- Alcock, C. *et al.* 1996, AJ, 111, 1146
- Arp, H. C. 1955, AJ, 60, 317
- Bailey, S. I. 1902, Harvard Ann. 38
- Bono, G., Caputo, F., Castellani, V. & Marconi, M. 1996, ApJ, 471, L33
- Bono, G., Caputo, F., Castellani, V. & Marconi, M. 1997, A&AS, 121, 327 (B97)
- Butler, D., Dickens, R. J. & Epps, E. 1978, ApJ, 225, 148
- Caputo, F. & Castellani, V. 1975, Ap&SS, 38, 39
- Clement, C., Dickens, R. J. & Bingham, E. 1979, AJ, 84, 217
- Clement, C. M. & Shelton, I. 1996, AJ, 112, 618
- Clement, C. M. & Shelton, I. 1997, AJ, 113, 1711
- Clement, C. M. & Shelton, I. 1999a, AJ, 118, 453
- Clement, C. M. & Shelton, I. 1999b, ApJ, 515, L85
- Clementini, G., Carretta, E., Gratton, R., Merighi, R., Mould, J. R., & McCarthy, J. K.
1995, AJ, 110, 2319
- Corwin, T. M., Carney, B. W. & Nifong, B. G. 1999, AJ, 118, 2875
- Cox, A. N. 1995, Astrophysical Applications of Powerful New Databases, ASP Conference
Ser 78, ed. S. J. Adelman & W. L. Wiese, 243
- Demarque, P., Zinn, R., Lee, Y.-W. & Yi, S. 2000, AJ, 119, 1398

- Demers, S. & Wehlau, A. 1977, *AJ*, 82, 620
- Dorman, B. 1992, *ApJS*, 81, 221
- Freeman, K. C. & Rodgers, A. W. 1975, *ApJ*, 201, L71
- Freyhammer, L. M., Andersen, M. I. & Petersen, J. O. 1998, *A Half Century of Stellar Pulsation Interpretations*, ASP Conference Ser 135, ed. P. A. Bradley & J. A. Guzik, 458
- Freyhammer, L. M., Petersen, J. O. & Andersen, M. I. 2000, *IAU Coll. 176, The Impact of Large-Scale Surveys on Pulsating Star Research*, ASP Conference Ser 203, ed. L. Szabados, & D. W. Kurtz, 252
- Gratton, R. G., Tornambè, A. & Ortolani, S. 1986, *A&A*, 169, 111
- Hilker, M. & Richtler, T. 1999, *astro-ph/9910370*
- Hughes, J. & Wallerstein, G. 2000, *AJ*, 119, 1225
- Jurcsik, J. 1998a, *ApJ*, 506, L113
- Jurcsik, J. 1998b, *A&A*, 333, 571
- Jurcsik, J. 2000, *IAU Coll. 176, The Impact of Large-Scale Surveys on Pulsating Star Research*, ASP Conference Ser 203, ed. L. Szabados, & D. W. Kurtz, 254
- Jurcsik, J., Clement, C., Geyer, H. & Domsa, I. 2000, *AJ*, (submitted)
- Jurcsik, J. & Kovács, G. 1996, *A&A*, 312, 111 (JK)
- Kaluzny, J., Hilditch, R., Clement, C. & Rucinski, S. M. 1998, *MNRAS*, 296, 347 (K98)
- Kaluzny, J., Kubiak, M., Szymański, A., Udalski, A., Krzemiński, W. & Mateo, M. 1996, *A&AS*, 120, 139

- Kaluzny, J., Kubiak, M., Szymański, A., Udalski, A., Krzemiński, W., Mateo, M. & Stanek, K. 1997a, A&AS, 122, 471
- Kaluzny, J., Kubiak, M., Szymański, A., Udalski, A., Krzemiński, W. & Mateo, M. 1997b, A&AS, 125, 343 (K97b)
- Kaluzny, J., Olech, A., Thompson, I., Pych, W., Krzemiński, W. & Schwarzenberg-Czerny, A. 2000, A&AS, 143, 215 (K2000)
- Kinman, T. D. 1959, MNRAS, 119, 538
- Kiss, L. L., Csák, B., Thomson, J. R. & Vinkó, J. 1999, A&A, 345, 149
- Kovács, G., Buchler, J. R., Marom, A., Iglesias, C. A., & Rogers, F. J. 1992, A&A, 259, L46
- Kovács, G. 1998a, A Half Century of Stellar Pulsation Interpretations, ASP Conference Ser 135, ed. P. A. Bradley & J. A. Guzik, 52
- Kovács, G. 1998b, Mem. Soc. Astron. Italiana, 69, 49
- Kovács, G. & Jurcsik, J. 1996, ApJ, 466, L17
- Kovács, G. & Kanbur, S. M. 1998, MNRAS, 295, 834
- Kovács, G. *et al.* 2000, IAU Coll. 176, The Impact of Large-Scale Surveys on Pulsating Star Research, ASP Conference Ser 203, ed. L. Szabados, & D. W. Kurtz, 313
- Lee, J.-W. & Carney, B. W. 1999a, AJ, 117, 2868
- Lee, J.-W. & Carney, B. W. 1999b, AJ, 118, 1373
- Lee, Y.-W., Demarque, P. & Zinn, R. 1990, ApJ, 350, 155 (LDZ)
- Martin, W. C. 1938, Leiden Annals, 17, No. 2

- Moskalik, P. 2000, IAU Coll. 176, The Impact of Large-Scale Surveys on Pulsating Star Research, ASP Conference Ser 203, ed. L. Szabados, & D. W. Kurtz, 315
- Nemec, J. M., Nemec, A. F. L. & Norris, J. 1986, AJ, 92, 358
- Olech, A., Kaluzny, J., Thompson, I. B., Pych, W., Krzeminski, W. & Schwarzenberg-Czerny, A. 1999a, AJ, 118, 442
- Olech, A., Woźniak, P. R., Alard, C., Kaluzny, J. & Thompson, I. B. 1999b, MNRAS, 310, 759
- Oosterhoff, P. Th. 1939, Observatory, 62, 104
- Oosterhoff, P. Th. 1944, BAN, 10, 55
- Purdue, P., Silbermann, N. A., Gay, P. & Smoth, H. A. 1995, AJ, 110, 1712
- Rey, S.-C., Lee, Y.-L., Joo, J.-M., Walker, A. & Baird, S. 2000, AJ, 119, 1824 (R2000)
- Sandage, A. 1958, in Stellar Populations, ed. D. O’Connell (Amsterdam: North-Holland), 41.
- Sandage, A. 1993, AJ, 106, 703
- Sawyer Hogg, H. 1973, Publ. David Dunlap Obs., 3, No. 6
- Schwarzschild, M. 1940, Harvard Circular 437
- Silbermann, N. A. & Smith, H. A. 1995, AJ, 110, 704
- Simon, N. R. & Clement, C. M. 1993a, in New Perspectives on Stellar Pulsation and Pulsating Variable Stars, IAU Coll 139, ed. J. M. Nemec and J. M. Matthews, 315
- Simon, N. R. & Clement, C. M. 1993b, ApJ, 410, 526

Stellingwerf, R. F., Gautschy, A. & Dickens, R. J. 1987, ApJ, L75

van Albada, T. S. & Baker, N. 1973, ApJ, 185, 477

van Agt, S. & Oosterhoff, P. Th. 1959, Leiden Annals, 21, 253

Van Hoolst, T., Dziembowski, W. A. & Kawaler, S. D. 1998, MNRAS, 297, 536

Walker, A. 1994, AJ, 108, 555

Walker, A. & Nemec, J. M. 1996, AJ, 112, 2026

Zinn, R. 1985, ApJ, 293, 424

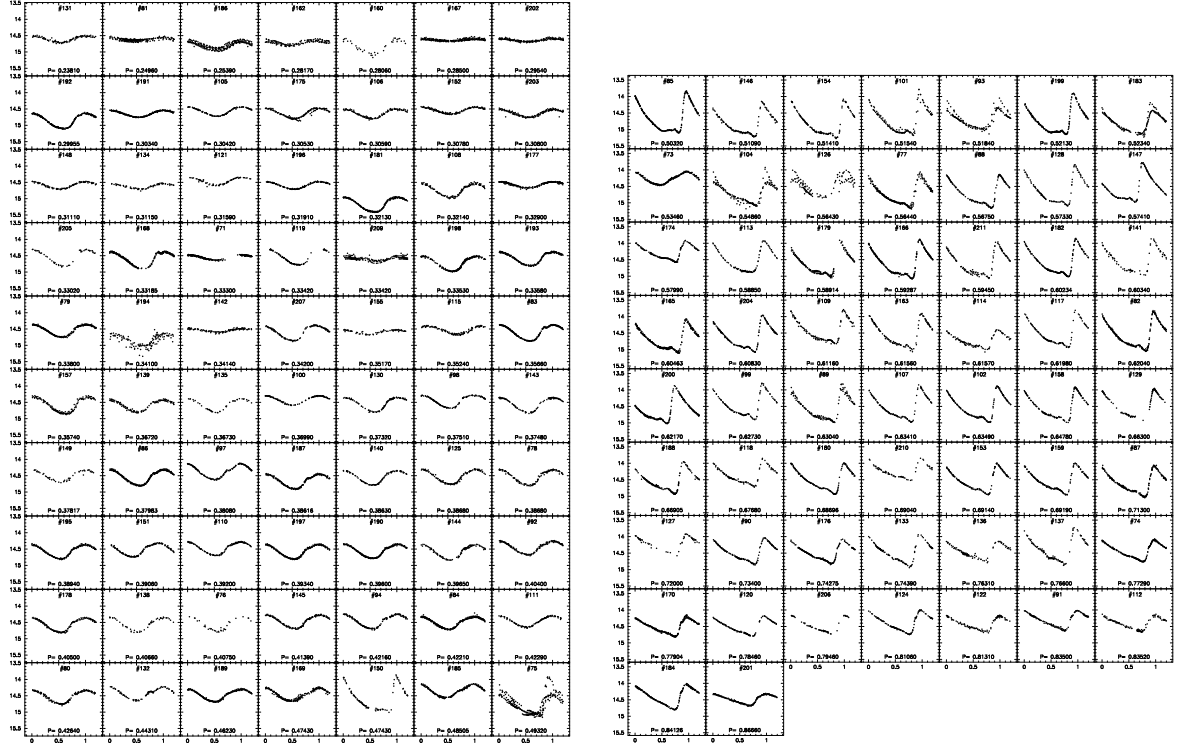


Fig. 1.— V light curves for the 128 stars in our sample. The curves are arranged in order of increasing period.

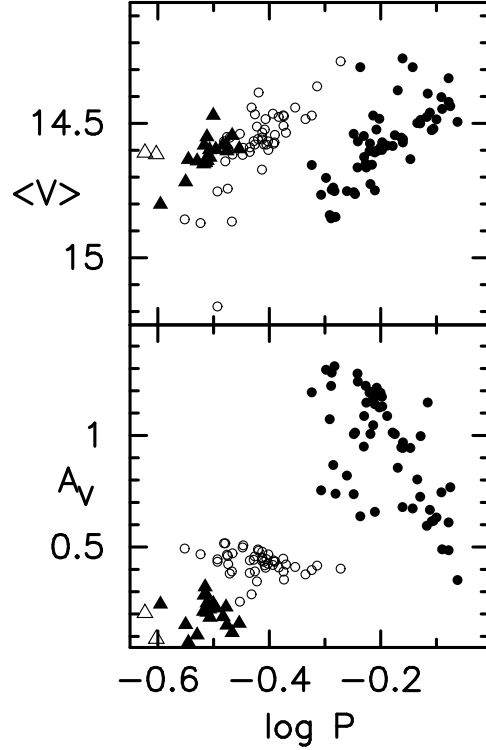


Fig. 2.— The period-luminosity and period-amplitude relation ($\langle V \rangle$ and A_V versus $\log P$) for the RR Lyrae variables in ω Cen. The points in the diagram fall into four different regimes which appear to correspond to different modes of pulsation and so we have plotted them with different symbols. The solid circles represent the fundamental mode, the open circles denote the first overtone, the solid triangles are the second overtone and the open triangles are the third overtone. Among the fundamental mode and second overtone pulsators, the P-A relation appears to be segregated into two groups according to luminosity. This occurs because stars of both Oosterhoff types are present in ω Cen.

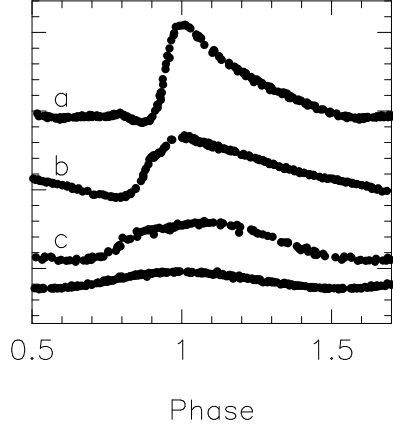


Fig. 3.— OGLE V light curves for the RR Lyrae variables Bailey (1902) considered to be the prototypes for his three subclasses. These are #199, (type a , $P=0^{\text{d}}5213$), #184 (type b , $P=0^{\text{d}}84126$) and #78 (type c , $P=0.3868$). Bailey type a and b variables pulsate in the fundamental mode, while type c variables pulsate in the first overtone. The bottom curve in the diagram is for #191 ($P=0^{\text{d}}3034$). There is a marked decrease in amplitude and increase in symmetry of the curves as one progresses through the Bailey subclasses and #191 is an extension of the sequence. We consider it to be a second overtone pulsator.

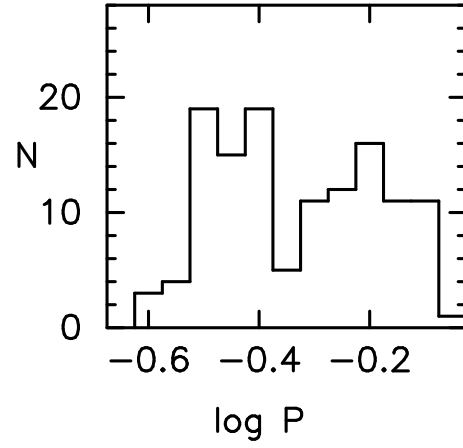


Fig. 4.— Period-frequency distribution for the RR Lyrae variables in the OGLE sample for ω Cen. The peak at $\log P = -0.5$ is due in part to the presence of second overtone pulsators (RRe stars).

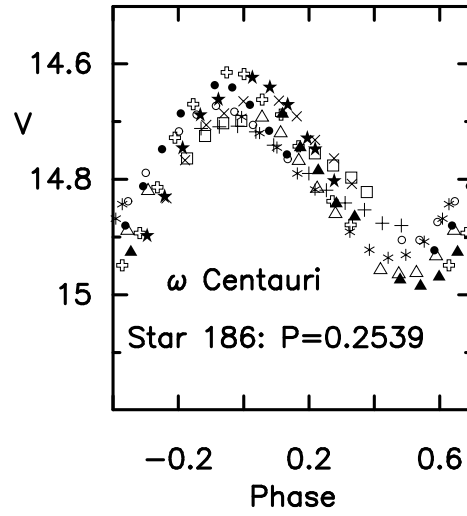


Fig. 5.— V light curve for OGLE #186 on 10 consecutive nights in 1995 (JD 2449821 to 2449830). Each night is plotted as a different symbol illustrating that the amplitude changes from cycle to cycle.

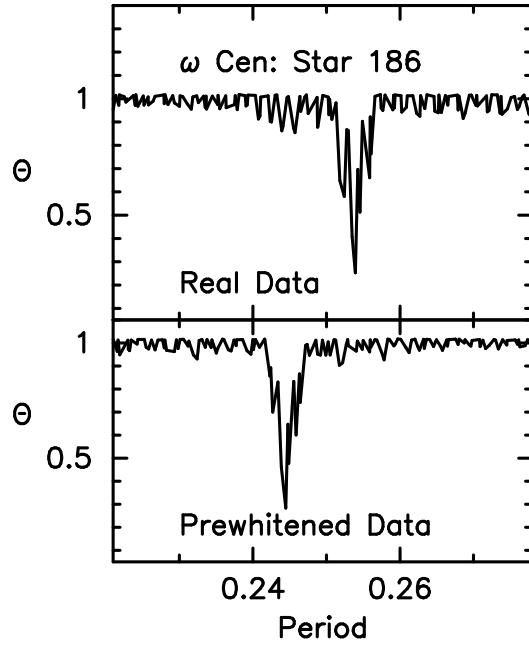


Fig. 6.— Θ -transforms for the real and prewhitened data for OGLE #186. In the upper panel, the minimum occurs at $0^{\text{d}}.2539$, the adopted period. After prewhitening with this period, the minimum Θ value is $0^{\text{d}}.2445$. This multiple periodicity is probably due to non-radial oscillations.

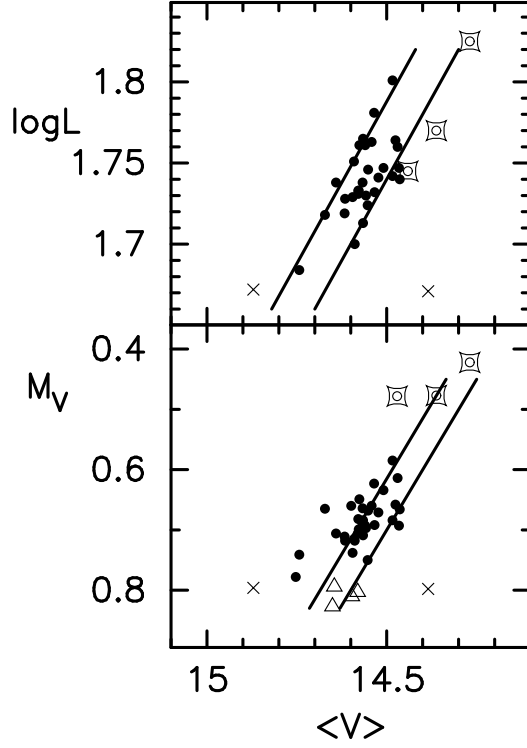


Fig. 7.— $\log L$ derived from equation (2) and M_V derived from equation (5) plotted against $\langle V \rangle$ for RRc stars (solid circles) and RRe stars (open triangles) in ω Cen. The open circles enclosed in boxes represent 4 stars that have anomalously high values of ϕ_{21} . Stars considered to be non-members are plotted as crosses. The envelope lines in the upper panel have a slope of 0.4 and are separated by $\Delta V = 0.12$ which represents the uncertainty of the fit of equation (2) to the models. The lines in the lower panel have a slope of unity and are separated by $\Delta V = 0.085$ the uncertainty in the calibration of equation (5).

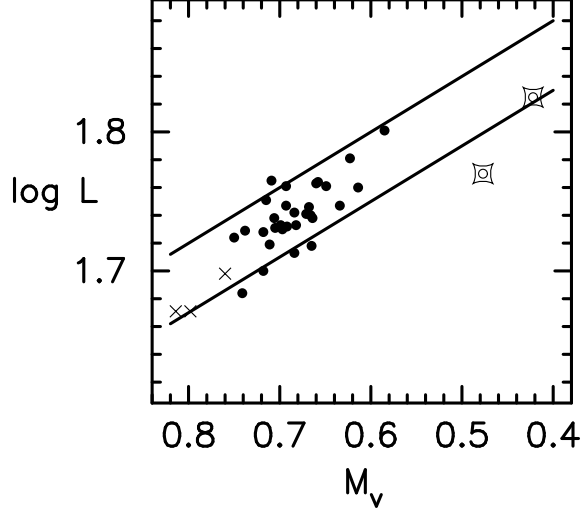


Fig. 8.— $\log L/L_\odot$ derived from equation (2) for the RRc stars in ω Cen. plotted against M_V derived from equation (5). The symbols are the same as in Fig. 7. The envelope lines have a slope of 0.4 and are separated by $\log L = 0.05$ which represents the uncertainty in the fit of the models to equation (2).

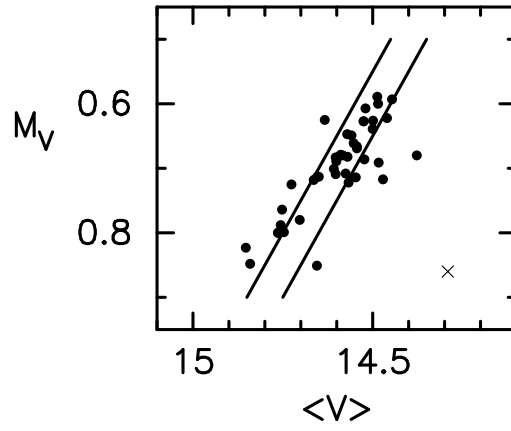


Fig. 9.— M_V calculated from equation (6) plotted against $\langle V \rangle$ for the RRab stars with ‘normal’ light curves. The cross represents #174 (V84) which is considered to be a non-member.

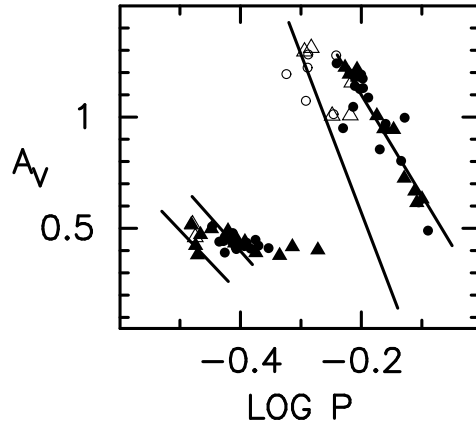


Fig. 10.— Period - V amplitude plot for selected fundamental mode and first overtone RR Lyrae variables in ω Cen. Among the fundamental mode variables, only the ones with ‘normal’ light curves are plotted. For the overtone pulsators, only those with an error less than 0.2 in ϕ_{31} are included. The circles represent the stars in field 5139B: solid circles for stars with $\langle V \rangle \leq 14.65$ and open circles for the fainter stars. The solid and open triangles represent stars brighter and fainter than 14.65 in other fields. Also included are lines delineating the P-A relations for RRc and RRab stars in OoI and OoII clusters. The two lines in the range of $\log P$ between -0.5 and -0.4 follow the P-A relation for RRc stars in the OoI cluster M3 and the OoII cluster M68. The two lines in the range of $\log P$ between -0.3 and -0.1 represent least squares fits to the P-A relation for OoI RRab stars in M3 and the OoII RRab stars in ω Cen, i.e. those with $\langle V \rangle \leq 14.65$.

Table 1. The RR Lyrae Variables in ω Centauri (OGLE data)

Ogle #	Sawyer Hogg #	Field	Period (days)	A_V	$\langle V \rangle$	Pulsation mode
71	185	A	0.3330	0.231	14.580	2nd
73	68	A	0.5346	0.403	14.269	1st
74	54	A	0.7729	0.667	14.460	F(n)
75	130	A	0.4932	0.754	14.766	F(p)
76	66	B	0.4075	0.435	14.543	1st
77	67	A	0.5644	1.006	14.756	F(n)
78	35	B	0.3868	0.479	14.552	1st
79	76	A	0.3380	0.381	14.553	1st
80	77	B	0.4264	0.422	14.535	1st
81		A	0.2496	0.089	14.615	3rd?
82	32	A	0.6204	1.214	14.603	F(n)
83	83	A	0.3566	0.498	14.617	1st
84	75	A	0.4221	0.390	14.509	1st
85	74	A	0.5032	1.294	14.703	F(n)
86	36	A	0.37983	0.489	14.558	1st
87	7	A	0.7130	0.944	14.633	F(n)
88	44	B	0.5675	1.013	14.763	F(n)
89	115	B	0.6304	1.191	14.589	F(n)
90	34	B	0.7340	0.803	14.499	F(n)
91	128	B	0.8350	0.610	14.332	F(p)
92	30	B	0.4040	0.420	14.464	1st
93	59	B	0.5184	0.868	14.739	F(p)
94	117	B	0.4216	0.448	14.470	1st

Table 1—Continued

Ogle #	Sawyer Hogg #	Field	Period (days)	A_V	$< V >$	Pulsation mode
97	21	B	0.3808	0.484	14.385	1st
98	10	B	0.3751	0.391	14.466	1st
99	4	B	0.6273	1.126	14.483	F(n)
100	58	B	0.3699	0.288	14.441	1st
101	5	B	0.5154	1.281	14.747	F(n)
102	122	B	0.6349	1.130	14.570	F(n)
104	120	B	0.5486	0.820	14.752	F(p)
105	121	B	0.3042	0.284	14.581	2nd
106	119	B	0.3059	0.292	14.646	2nd
107	40	B	0.6341	1.173	14.599	F(n)
108		B	0.3214	0.434	14.753	1st
109	118	B	0.6116	1.046	14.471	F(n)
110	131	B	0.3920	0.407	14.484	1st
111		B	0.4229	0.354	14.473	1st
112	144	B	0.8352	0.486	14.420	F(p)
113	25	B	0.5885	0.950	14.547	F(n)
114	27	B	0.6157	0.658	14.749	F(p)
115		B	0.3524	0.255	14.539	1st
117	62	B	0.6198	1.184	14.523	F(n)
118	139	B	0.6768	0.855	14.377	F(n)
119	137	B	0.3342	0.466	14.550	1st
120	26	B	0.7846	0.617	14.520	F(n)
121		B	0.3159	0.246	14.470	2nd

Table 1—Continued

Ogle #	Sawyer Hogg #	Field	Period (days)	A_V	$< V >$	Pulsation mode
122		B	0.8131	0.490	14.446	F(n)
124	15	B	0.8106	0.745	14.402	F(p)
125	12	B	0.3868	0.453	14.534	1st
126	11	B	0.5643	0.737	14.539	F(p)
127	116	B	0.7200	0.673	14.291	F(p)
128	113	B	0.5733	1.277	14.664	F(n)
129	41	B	0.6630	1.013	14.584	F(p)
130	145	B	0.3732	0.443	14.566	1st
131		B	0.2381	0.204	14.609	3rd?
132		B	0.4431	0.411	14.441	1st
133	109	B	0.7439	0.997	14.487	F(n)
134		B	0.3115	0.185	14.626	2nd
135	158	B	0.3673	0.440	14.589	1st
136	111	B	0.7631	0.595	14.476	F(p)
137	99	B	0.7660	1.148	14.389	F(p)
138	157	B	0.4066	0.435	14.571	1st
139		B	0.3672	0.384	14.606	1st
140	153	B	0.3863	0.438	14.560	1st
141	90	B	0.6034	1.196	14.575	F(n)
142	166	B	0.3414	0.117	14.545	2nd
143	89	B	0.3748	0.458	14.579	1st
144	87	B	0.3965	0.467	14.599	1st
145	155	B	0.4139	0.409	14.476	1st

Table 1—Continued

Ogle #	Sawyer Hogg #	Field	Period (days)	A_V	$< V >$	Pulsation mode
146	23	B	0.5109	1.073	14.841	F(n)
147	51	B	0.5741	1.241	14.567	F(n)
148		B	0.3111	0.222	14.598	2nd
149		B	0.378175	0.346	14.512	1st
150	112	B	0.4743	1.193	14.655	F(n)
151	70	B	0.3906	0.418	14.523	1st
152		B	0.3078	0.208	14.550	2nd
153	102	B	0.6914	0.944	14.571	F(n)
154	107	B	0.5141	1.222	14.853	F(n)
155		B	0.3517	0.158	14.595	2nd
157	71	B	0.3574	0.508	14.591	1st
158	86	B	0.6478	1.087	14.583	F(n)
159	97	B	0.6919	0.969	14.559	F(n)
160	98	B	0.2806	0.493	14.857	1st
162		B	0.2817	0.153	14.718	2nd
163	20	B	0.6156	1.140	14.608	F(n)
165	49	C	0.60463	1.007	14.726	F(n)
166	125	C	0.59287	1.223	14.650	F(n)
167		C	0.2850	0.073	14.634	2nd
168	124	C	0.33185	0.517	14.641	1st
169	123	C	0.4743	0.397	14.471	1st
170	38	C	0.77904	0.615	14.525	F(n)
174	84	D	0.5799	0.638	14.291	F(n)

Table 1—Continued

Ogle #	Sawyer Hogg #	Field	Period (days)	A_V	$< V >$	Pulsation mode
175	127	D	0.3053	0.321	14.640	2nd
176	85	D	0.74275	0.725	14.500	F(n)
177		D	0.3290	0.188	14.580	2nd
178	95	D	0.4050	0.440	14.576	1st
179	45	D	0.58914	1.087	14.625	F(p)
180	46	D	0.68696	0.947	14.553	F(n)
181	168	D	0.3213	0.445	15.181	1st
182	33	D	0.60234	1.192	14.603	F(n)
183	9	BC	0.5234	0.739	14.848	F(p)
184	3	D	0.84126	0.768	14.436	F(p)
185	47	D	0.48505	0.417	14.362	1st
186		D	0.2539	0.244	14.801	2nd
187	50	D	0.38616	0.450	14.672	1st
188	13	D	0.66905	1.006	14.544	F(n)
189	24	E	0.4623	0.378	14.484	1st
190	22	E	0.3960	0.425	14.567	1st
191	184	E	0.3034	0.212	14.651	2nd
192	19	E	0.29955	0.468	14.871	1st
193	82	E	0.3358	0.423	14.595	1st
194	101	E	0.3410	0.391	14.865	1st
195	81	E	0.3894	0.434	14.578	1st
196		B	0.3191	0.227	14.597	2nd
197	39	E	0.3934	0.446	14.579	1st

Table 1—Continued

Ogle #	Sawyer Hogg #	Field	Period (days)	A_V	$< V >$	Pulsation mode
198	105	E	0.3353	0.460	14.743	1st
199	8	E	0.5213	1.310	14.752	F(n)
200	18	E	0.6217	1.179	14.601	F(n)
201	104	E	0.8666	0.352	14.494	F(p)
202		E	0.2954	0.106	14.640	2nd
203		E	0.3080	0.250	14.638	2nd
204	79	E	0.6083	1.155	14.654	F(n)
205	16	F	0.3302	0.517	14.566	1st
206	57	F	0.7946	0.632	14.485	F(n)
207	126	F	0.3420	0.472	14.616	1st
209		BC	0.3342	0.150	14.602	2nd
210	88	BC	0.6904	0.679	14.258	F(p)
211	108	BC	0.5945	1.147	14.664	F(p)

Table 2. Fourier Parameters for the Overtone Pulsators in ω Centauri

Ogle #	$\log P$	$\phi_{21}(\sigma)$	$\phi_{31}(\sigma)$	A_4	M_V	$\log L/L_\odot$	M/M_\odot	$[\text{Fe}/\text{H}]_{hk}$
131	-0.623	5.03 (0.37)	4.45 (0.50)	0.00626				
81	-0.603	3.00 (0.34)	6.99 (1.11)	0.00221				
186	-0.595	4.09 (0.32)	6.74 (3.75)	0.00295				
160	-0.552	4.21 (0.27)	4.49 (0.98)	0.01091				-1.05
162	-0.550	5.99 (0.52)	7.50 (2.79)	0.00180				
167	-0.545	4.93 (0.72)	4.94 (1.07)	0.00136				
202	-0.530	3.96 (0.52)	8.21 (0.77)	0.00396				
192	-0.524	4.66 (0.03)	3.34 (0.12)	0.00936	0.80	1.67	0.56	-1.22
191	-0.518	4.68 (0.10)	3.38 (0.56)	0.00123	0.83			
105	-0.517	4.81 (0.11)	3.81 (0.51)	0.00528	0.80			-1.46
175	-0.515	4.87 (0.23)	4.60 (0.35)	0.00505				-1.59
106	-0.514	5.02 (0.18)	3.53 (0.28)	0.00483	0.79			-1.61
152	-0.512	4.47 (0.24)	2.75 (0.71)	0.00075				
203	-0.511	4.80 (0.24)	7.66 (0.74)	0.00313				
148	-0.507	4.30 (0.33)	3.54 (0.40)	0.00094				
134	-0.507	4.85 (0.23)	4.24 (2.19)	0.00475				
121	-0.501	5.57 (0.56)	2.71 (0.51)	0.00373				
196	-0.496	4.78 (0.18)	2.67 (0.53)	0.00067	0.81			
181	-0.493	4.81 (0.04)	3.43 (0.05)	0.01112	0.76	1.70	0.57	
108	-0.493	4.67 (0.16)	3.96 (0.24)	0.00859	0.78			
177	-0.483	4.62 (0.32)	2.33 (0.63)	0.00377				
205*	-0.481	4.97 (0.10)	3.38 (0.15)	0.02481	0.68	1.71	0.59	-1.29
168*	-0.479	4.82 (0.04)	2.99 (0.07)	0.02084	0.71	1.74	0.65	-1.33

Table 2—Continued

Ogle #	$\log P$	$\phi_{21}(\sigma)$	$\phi_{31}(\sigma)$	A_4	M_V	$\log L/L_\odot$	M/M_\odot	$[\text{Fe}/\text{H}]_{hk}$
209	-0.476	4.93 (0.24)	7.08 (1.00)	0.00797				
198*	-0.475	5.13 (0.09)	4.00 (0.10)	0.00921	0.74	1.68	0.51	-1.24
193*	-0.474	4.92 (0.04)	3.24 (0.08)	0.01198	0.74	1.73	0.61	-1.56
79*	-0.471	5.02 (0.07)	3.38 (0.14)	0.00778	0.75	1.72	0.59	-1.45
194	-0.467	5.37 (0.52)	3.02 (0.75)	0.02575				-1.88
142	-0.467	5.19 (0.38)	4.42 (0.79)	0.00215				
207*	-0.466	4.98 (0.05)	3.41 (0.08)	0.01446	0.72	1.73	0.59	-1.31
155	-0.454	5.84 (0.54)	4.76 (0.35)	0.00399				
115	-0.453	4.91 (0.26)	2.07 (0.63)	0.00536				
83**	-0.448	4.92 (0.03)	3.89 (0.04)	0.01343	0.71	1.72	0.54	-1.30
157**	-0.447	4.78 (0.11)	3.35 (0.17)	0.01371	0.72	1.75	0.62	
139	-0.435	5.64 (0.21)	4.11 (0.21)	0.00932				
135**	-0.435	5.45 (0.14)	4.44 (0.19)	0.00441	0.72	1.70	0.47	-1.25
100	-0.432	5.74 (0.22)	5.00 (1.24)	0.00305				-1.37
130**	-0.428	5.15 (0.08)	3.44 (0.15)	0.00817	0.71	1.77	0.62	-1.58
143**	-0.426	5.32 (0.08)	4.07 (0.12)	0.00693	0.71	1.73	0.53	-1.37
98**	-0.426	5.39 (0.04)	3.79 (0.07)	0.00896	0.69	1.75	0.56	-1.66
149	-0.422	5.37 (0.54)	3.77 (0.52)	0.01088				
86**	-0.420	4.92 (0.07)	4.18 (0.08)	0.01154	0.70	1.73	0.52	-1.49
97	-0.419	2.48 (0.21)	5.22 (0.09)	0.01279	0.80	1.67	0.40	-0.90
187**	-0.413	5.43 (0.07)	4.52 (0.10)	0.01227	0.67	1.72	0.48	-1.59
140**	-0.413	5.24 (0.08)	3.79 (0.11)	0.00804	0.69	1.76	0.57	-1.38
125**	-0.413	4.89 (0.19)	4.30 (0.17)	0.01157	0.69	1.73	0.50	-1.53

Table 2—Continued

Ogle #	$\log P$	$\phi_{21}(\sigma)$	$\phi_{31}(\sigma)$	A_4	M_V	$\log L/L_\odot$	M/M_\odot	$[\text{Fe}/\text{H}]_{hk}$
78**	-0.413	5.16 (0.13)	4.05 (0.15)	0.01419	0.67	1.75	0.54	-1.56
195**	-0.410	5.06 (0.08)	4.33 (0.10)	0.00759	0.70	1.73	0.50	-1.72
151**	-0.408	5.46 (0.10)	4.21 (0.07)	0.00975	0.67	1.74	0.52	-1.94
110**	-0.407	5.24 (0.09)	4.23 (0.10)	0.00881	0.68	1.74	0.52	-1.56
197**	-0.405	5.16 (0.08)	4.41 (0.09)	0.00957	0.68	1.73	0.50	-1.96
190**	-0.402	5.38 (0.08)	4.38 (0.07)	0.01098	0.66	1.74	0.50	-1.93
144	-0.402	5.10 (0.18)	3.96 (0.21)	0.00899	0.69			-1.44
92**	-0.394	5.32 (0.18)	4.50 (0.15)	0.00945	0.67	1.74	0.49	-1.75
178**	-0.393	5.39 (0.11)	4.15 (0.13)	0.01237	0.65	1.76	0.54	-1.84
138	-0.391	5.23 (0.53)	4.32 (0.40)	0.01146				-1.49
76**	-0.390	5.37 (0.10)	4.16 (0.10)	0.00957	0.66	1.76	0.54	-1.68
145**	-0.383	5.29 (0.11)	4.26 (0.13)	0.00928	0.66	1.76	0.53	-1.46
94**	-0.375	5.49 (0.12)	4.48 (0.10)	0.01571	0.61	1.76	0.50	-1.68
84**	-0.375	5.88 (0.12)	4.71 (0.13)	0.00713	0.63	1.75	0.48	-1.49
111	-0.374	5.42 (0.48)	5.12 (0.68)	0.00454				
80**	0.370	5.60 (0.12)	4.20 (0.17)	0.01143	0.62	1.78	0.54	-1.81
132	-0.354	7.50 (0.37)	5.13 (0.13)	0.01449		1.745	0.44	
189	-0.335	6.33 (0.09)	4.49 (0.08)	0.00508	0.59	1.80	0.53	
169	-0.324	8.35 (0.14)	5.48 (0.23)	0.00648	0.48			-1.64
185	-0.314	8.10 (0.12)	5.40 (0.12)	0.00692	0.48	1.77	0.43	-1.58
73	-0.272	8.38 (0.09)	5.21 (0.08)	0.00573	0.42	1.83	0.47	-1.60

Table 3. Fourier Parameters for RRab Stars in ω Centauri

Ogle #	$\log P$	A_1	$\phi_{31}(\sigma)$	M_V	$[\text{Fe}/\text{H}]_{hk}$
150	-0.324	0.392	1.51	0.85	-1.81
85	-0.298	0.465	1.55	0.78	-1.83
146	-0.292	0.364	1.85	0.85	-1.08
154	-0.289	0.399	1.81	0.82	-1.36
101	-0.288	0.441	1.79	0.80	-1.35
199	-0.283	0.452	1.58	0.76	-1.91
77	-0.248	0.358	1.96	0.79	-1.10
88	-0.246	0.343	2.05	0.80	-1.40
128	-0.242	0.437	1.77	0.72	-1.65
147	-0.241	0.426	1.77	0.72	-1.64
174	-0.237	0.239	2.32	0.86	-1.47
113	-0.230	0.396	1.75	0.71	-1.57
166	-0.227	0.414	1.88	0.71	-1.67
182	-0.220	0.398	1.90	0.71	-2.09
141	-0.219	0.398	1.90	0.71	-2.21
165	-0.219	0.344	1.83	0.73	-1.98
204	-0.216	0.391	1.98	0.71	-1.39
109	-0.214	0.349	1.87	0.72	-1.62
163	-0.211	0.391	1.97	0.70	
117	-0.208	0.399	1.91	0.69	-1.62
82	-0.207	0.407	1.93	0.68	-1.53
200	-0.206	0.396	1.95	0.69	-1.78
99	-0.203	0.381	1.98	0.69	-1.74

Table 3—Continued

Ogle #	$\log P$	A_1	$\phi_{31}(\sigma)$	M_V	$[\text{Fe}/\text{H}]_{hk}$
89	-0.200	0.385	1.93	0.68	-1.87
107	-0.198	0.379	2.00	0.68	-1.60
102	-0.197	0.376	1.98	0.68	-2.02
158	-0.189	0.360	2.06	0.68	-1.81
188	-0.175	0.365	2.31	0.67	-1.91
118	-0.170	0.289	2.12	0.68	-1.46
180	-0.163	0.323	2.23	0.66	-1.88
153	-0.160	0.328	2.18	0.65	-1.84
159	-0.160	0.330	2.21	0.65	-1.56
87	-0.147	0.328	2.26	0.63	-1.46
90	-0.134	0.287	2.36	0.63	-1.71
176	-0.129	0.270	2.53	0.64	-1.87
133	-0.129	0.355	2.45	0.59	-1.51
74	-0.112	0.250	2.68	0.62	-1.66
170	-0.108	0.230	2.72	0.63	-1.75
120	-0.105	0.237	2.63	0.61	-1.68
206	-0.100	0.228	2.66	0.60	-1.89
122	-0.090	0.192	2.67	0.59	

Table 4. Derived Parameters for RRc Stars of Different Oosterhoff Types

Cluster	[Fe/H]	No. of Stars	mean P (days)	Oosterhoff type	mean M/M_{\odot}	mean $\log L/L_{\odot}$	mean T_{eff}
M107 (N6171)	-0.99	6	0.292	I	0.54 ± 0.01	1.65 ± 0.01	7448 ± 19
M5	-1.40	14	0.324	I	0.54 ± 0.02	1.69 ± 0.01	7353 ± 19
M3	-1.66	5	0.325	I	0.59 ± 0.03	1.71 ± 0.01	7315 ± 7
ω Cen	(-1.36)	6	0.336	I	0.59 ± 0.02	1.72 ± 0.01	7287 ± 12
ω Cen	(-1.60)	23	0.391	II	0.53 ± 0.01	1.74 ± 0.005	7199 ± 8
M55	-1.82	5	0.391	II	0.53 ± 0.01	1.75 ± 0.01	7193 ± 12
M68	-2.09	16	0.369	II	0.71 ± 0.01	1.79 ± 0.01	7145 ± 18
M15	-2.15	6	0.367	II	0.73 ± 0.02	1.80 ± 0.01	7136 ± 31

Table 5. Mass Differences for Pairs of RRab Stars in ω Centauri

Stars	$\Delta \log P$	ΔV	ΔA_V	$\Delta[\text{Fe}/\text{H}]$	$\Delta \log M/M_\odot$	$\Delta \log M/M_\odot$	$\Delta \log M/M_\odot$
OoI, OoII	(II-I)	(II-I)	(II-I)	(II-I)	$(\Delta T = 0.000)^\dagger$	$(\Delta T = -0.004)^\dagger$	$(\Delta T = -0.005)^\dagger$
150, 141	0.1046	-0.080	0.003	-0.60	-0.107	-0.089	-0.077
150, 117	0.1162	-0.132	-0.009	-0.11	-0.110	-0.091	-0.080
146, 158	0.1031	-0.258	0.014	-0.73	-0.009	+0.003	+0.015
154, 147	0.0479	-0.286	0.019	-0.28	+0.079	+0.093	+0.105
101, 128	0.0462	-0.083	0.004	-0.30	-0.022	-0.005	+0.008
88, 133	0.1175	-0.276	-0.016	-0.11	-0.037	-0.022	-0.011
113, 153	0.0700	+0.024	-0.006	-0.27	-0.114	-0.096	-0.083
mean	0.0865	-0.156		-0.34	-0.046	-0.030	-0.018

$^\dagger \Delta T$ refers to $\Delta \log T_e$